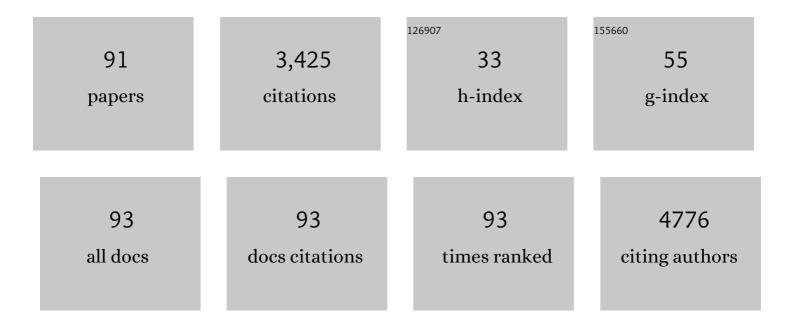
List of Publications by Year in descending order

Source: https://exaly.com/author-pdf/4126542/publications.pdf Version: 2024-02-01



NAME

#	Article	IF	CITATIONS
1	Dual synergistic effects between Co and Mo2C in Co/Mo2C heterostructure for electrocatalytic overall water splitting. Chemical Engineering Journal, 2022, 430, 132697.	12.7	91
2	Activation engineering on metallic 1T-MoS2 by constructing In-plane heterostructure for efficient hydrogen generation. Applied Catalysis B: Environmental, 2022, 300, 120696.	20.2	60
3	A Photoelectrochemical Platform Based on Polyaniline-Modified Titanium Dioxide Facet Heterostructure. ACS Applied Bio Materials, 2022, 5, 1297-1304.	4.6	1
4	Iron doped mesoporous cobalt phosphide with optimized electronic structure for enhanced hydrogen evolution. International Journal of Hydrogen Energy, 2022, 47, 14767-14776.	7.1	17
5	Ni(OH)2 nanoparticles decorated on 1T phase MoS2 basal plane for efficient water splitting. Applied Surface Science, 2022, 593, 153408.	6.1	10
6	1T-MoS ₂ Nanosheets Coupled with CoS ₂ Nanoparticles: Electronic Modulation for Efficient Electrochemical Nitrogen Fixation. Inorganic Chemistry, 2022, 61, 7608-7616.	4.0	7
7	Unveiling the relationship between the multilayer structure of metallic MoS ₂ and the cycling performance for lithium ion batteries. Nanoscale, 2022, 14, 8621-8627.	5.6	9
8	Dual Stimuli-Responsive Inks Based on Orthogonal Upconversion Three-Primary-Color Luminescence for Advanced Anticounterfeiting Applications. , 2022, 4, 1306-1313.		24
9	Boosted hydrogen evolution reaction based on synergistic effect of RuO2@MoS2 hybrid electrocatalyst. Applied Surface Science, 2021, 538, 148019.	6.1	21
10	Symbiotic composite composed of MoS2 and pelagic clay with enhanced disinfection efficiency. RSC Advances, 2021, 11, 9621-9627.	3.6	5
11	Supramolecular complex strategy for pure organic multi-color luminescent materials and stimuli-responsive luminescence switching. CrystEngComm, 2021, 23, 5918-5924.	2.6	10
12	Electrochemical Fixation of Nitrogen by Promoting N ₂ Adsorption and N–N Triple Bond Cleavage on the CoS ₂ /MoS ₂ Nanocomposite. ACS Applied Materials & Interfaces, 2021, 13, 21474-21481.	8.0	39
13	Ultra-small NiFe-layered double hydroxide nanoparticles confined in ordered mesoporous carbon as efficient electrocatalyst for oxygen evolution reaction. Applied Surface Science, 2021, 565, 150533.	6.1	17
14	Three-Dimensional Ordered Macroporous NiFe ₂ O ₄ Self-Supporting Electrode with Enhanced Mass Transport for High-Efficiency Oxygen Evolution Reaction. ACS Applied Energy Materials, 2021, 4, 268-274.	5.1	14
15	Self-Propelled Nanojets for Fenton Catalysts Based on Halloysite with Embedded Pt and Outside-Grafted Fe ₃ O ₄ . ACS Applied Materials & Interfaces, 2021, 13, 49017-49026.	8.0	14
16	Hydrothermal Synthesis of 1T-MoS2/Pelagic Clay Composite and Its Application in the Catalytic Reduction of 4-Nitrophenol. Materials, 2021, 14, 7020.	2.9	6
17	Ultrafine Cobaltâ€Đoped Iron Disulfide Nanoparticles in Ordered Mesoporous Carbon for Efficient Hydrogen Evolution. ChemCatChem, 2020, 12, 788-794.	3.7	15
18	Self‣upported Mesoporous Iron Phosphide with High Active‣ite Density for Electrocatalytic Hydrogen Evolution in Acidic and Alkaline Media. ChemElectroChem, 2020, 7, 4943-4948.	3.4	10

#	Article	IF	CITATIONS
19	Periodically ordered mesoporous iron phosphide for highly efficient electrochemical hydrogen evolution. Journal of Colloid and Interface Science, 2020, 569, 68-75.	9.4	11
20	Selfâ€assembly Mesoporous FeP Film with High Porosity for Efficient Hydrogen Evolution Reaction. ChemCatChem, 2020, 12, 2589-2594.	3.7	11
21	1T- and 2H-mixed phase MoS2 nanosheets coated on hollow mesoporous TiO2 nanospheres with enhanced photocatalytic activity. Journal of Colloid and Interface Science, 2020, 567, 10-17.	9.4	29
22	Enhanced Iridium Mass Activity of 6H-Phase, Ir-Based Perovskite with Nonprecious Incorporation for Acidic Oxygen Evolution Electrocatalysis. ACS Applied Materials & Interfaces, 2019, 11, 42006-42013.	8.0	48
23	Vertical nanosheet array of 1T phase MoS2 for efficient and stable hydrogen evolution. Applied Catalysis B: Environmental, 2019, 246, 296-302.	20.2	122
24	Co Doping and 1T Phase Jointly Enhanced HER Activity for Co-1T/2H MoS2. IOP Conference Series: Earth and Environmental Science, 2019, 267, 022044.	0.3	2
25	Ultra‧mall Molybdenum Carbide Nanoparticles inâ€situ Entrapped in Mesoporous Carbon Spheres as Efficient Catalysts for Hydrogen Evolution. ChemCatChem, 2019, 11, 2643-2648.	3.7	18
26	Three-dimensionally ordered macroporous FeP self-supported structure for high-efficiency hydrogen evolution reaction. International Journal of Hydrogen Energy, 2019, 44, 5854-5862.	7.1	16
27	Mesoporous carbon nanospheres deposited onto D-shaped fibers for femtosecond pulse generation. RSC Advances, 2019, 9, 11621-11626.	3.6	10
28	Defect-rich O-incorporated 1T-MoS2 nanosheets for remarkably enhanced visible-light photocatalytic H2 evolution over CdS: The impact of enriched defects. Applied Catalysis B: Environmental, 2018, 229, 227-236.	20.2	176
29	Synthesis of hierarchically meso-macroporous TiO2/CdS heterojunction photocatalysts with excellent visible-light photocatalytic activity. Journal of Colloid and Interface Science, 2018, 512, 47-54.	9.4	77
30	Tunable mid-infrared Raman soliton generation from 1.96 to 2.82 μm in an all-solid fluorotellurite fiber. AIP Advances, 2018, 8, .	1.3	23
31	Threeâ€Ðimensional Cathode Constructed through Confinedâ€Growth of FeP Nanocrystals in Ordered Mesoporous Carbon Film Coated on Carbon Cloth for Efficient Hydrogen Production. ChemCatChem, 2018, 10, 3441-3446.	3.7	7
32	Coherent supercontinuum generation from 1.4 to 4 <i>μ</i> m in a tapered fluorotellurite microstructured fiber pumped by a 1980 nm femtosecond fiber laser. Applied Physics Letters, 2017, 110, .	3.3	26
33	Plasmonic Cu _{1.8} S nanocrystals as saturable absorbers for passively Q-switched erbium-doped fiber lasers. Journal of Materials Chemistry C, 2017, 5, 4034-4039.	5.5	31
34	In situ synthesis of concentric C@MoS2 core–shell nanospheres as anode for lithium ion battery. Journal of Materials Science, 2017, 52, 13183-13191.	3.7	22
35	Heterogeneous Nanostructure Based on 1T-Phase MoS ₂ for Enhanced Electrocatalytic Hydrogen Evolution. ACS Applied Materials & Interfaces, 2017, 9, 25291-25297.	8.0	202
36	Synthesis of CdS/m-TiO2 mesoporous spheres and their application in photocatalytic degradation of rhodamine B under visible light. Chemical Research in Chinese Universities, 2017, 33, 436-441.	2.6	11

#	Article	IF	CITATIONS
37	Watermelon-like Rh x S y @C nanospheres: phase evolution and its influence on the electrocatalytic performance for oxygen reduction reaction. Journal of Materials Science, 2017, 52, 11402-11412.	3.7	5
38	Dual-wavelength mode-locked thulium-doped fiber laser based on carbon nanotube. , 2016, , .		0
39	High-efficiency hydrogen evolution reaction catalyzed by iron phosphide nanocrystals. RSC Advances, 2016, 6, 114430-114435.	3.6	16
40	Effect of the TMCS/hydrogel volume ratio on physical properties of silica aerogels based on fly ash acid sludge. Journal of Sol-Gel Science and Technology, 2016, 78, 279-284.	2.4	7
41	Tunable dual-wavelength passively mode-locked thulium-doped fiber laser using carbon nanotube. Optical Engineering, 2016, 55, 106115.	1.0	12
42	Effect of surface modification on physical properties of silica aerogels derived from fly ash acid sludge. Colloids and Surfaces A: Physicochemical and Engineering Aspects, 2016, 490, 200-206.	4.7	46
43	Hydrothermal synthesis of highly crystalline RuS2 nanoparticles as cathodic catalysts in the methanol fuel cell and hydrochloric acid electrolysis. Materials Research Bulletin, 2015, 65, 110-115.	5.2	29
44	Heterostructures of Ag 3 PO 4 /TiO 2 mesoporous spheres with highly efficient visible light photocatalytic activity. Journal of Colloid and Interface Science, 2015, 450, 246-253.	9.4	55
45	In situ synthesis of well crystallized rhodium sulfide/carbon composite nanospheres as catalyst for hydrochloric acid electrolysis. Journal of Materials Chemistry A, 2014, 2, 1484-1492.	10.3	14
46	Hierarchical tubular structure constructed by mesoporous TiO2 nanosheets: Controlled synthesis and applications in photocatalysis and lithium ion batteries. Chemical Engineering Journal, 2013, 232, 356-363.	12.7	23
47	Electrospinning of magnetical bismuth ferrite nanofibers with photocatalytic activity. Ceramics International, 2013, 39, 3511-3518.	4.8	83
48	Spherical Rh17S15@C and Rh@C core–shell nanocomposites: Synthesis, growth mechanism and methanol tolerance in oxygen reduction reaction. Chemical Engineering Journal, 2013, 228, 45-53.	12.7	10
49	Magnetically separable Fe3O4@SiO2@TiO2-Ag microspheres with well-designed nanostructure and enhanced photocatalytic activity. Journal of Hazardous Materials, 2013, 262, 404-411.	12.4	132
50	Effect of large pore size of multifunctional mesoporous microsphere on removal of heavy metal ions. Journal of Hazardous Materials, 2013, 254-255, 157-165.	12.4	128
51	Phosphotungstic acid anchored to amino–functionalized core–shell magnetic mesoporous silica microspheres: A magnetically recoverable nanocomposite with enhanced photocatalytic activity. Journal of Colloid and Interface Science, 2013, 390, 70-77.	9.4	45
52	Preparation of magnetically recoverable Fe3O4@SiO2@meso-TiO2 nanocomposites with enhanced photocatalytic ability. Materials Research Bulletin, 2012, 47, 2396-2402.	5.2	64
53	Synthesis of Fe3O4@SiO2–Ag magnetic nanocomposite based on small-sized and highly dispersed silver nanoparticles for catalytic reduction of 4-nitrophenol. Journal of Colloid and Interface Science, 2012, 383, 96-102.	9.4	281
54	Facile encapsulation of monodispersed silver nanoparticles in mesoporous compounds. Chemical Engineering Journal, 2012, 195-196, 254-260.	12.7	24

#	Article	IF	CITATIONS
55	Nanopores with Solvent-Sensitive Polymer Brushes: A Dissipative Particle Dynamics Simulation. Journal of Macromolecular Science - Physics, 2012, 51, 275-287.	1.0	9
56	Synthesis and growth mechanism of monodispersed MoS2 sheets/carbon microspheres. CrystEngComm, 2012, 14, 3027.	2.6	17
57	In situ auto-reduction of silver nanoparticles in mesoporous carbon with multifunctionalized surfaces. Journal of Materials Chemistry, 2012, 22, 13571.	6.7	40
58	Comprehensive study of mesoporous carbon functionalized with carboxylate groups and magnetic nanoparticles as a promising adsorbent. Journal of Colloid and Interface Science, 2012, 369, 366-372.	9.4	51
59	Study on a type of mesoporous silica humidity sensing material. Sensors and Actuators B: Chemical, 2012, 166-167, 658-664.	7.8	34
60	Synthesis, Characterization, and Humidity Sensing Property of Mesoporous Cerium Oxide. Journal of Nanoengineering and Nanomanufacturing, 2012, 2, 41-45.	0.3	1
61	Humidity sensing properties of mesoporous iron oxide/silica composite prepared via hydrothermal process. Sensors and Actuators B: Chemical, 2011, 160, 334-340.	7.8	48
62	Sub-micrometer sized yttrium oxide fibers prepared through hydrothermal reaction. Materials Research Bulletin, 2011, 46, 428-431.	5.2	9
63	TiO2 supported on rod-like mesoporous silica SBA-15: Preparation, characterization and photocatalytic behaviour. Materials Research Bulletin, 2011, 46, 2317-2322.	5.2	19
64	Controlling electroosmotic flow by polymer coating: a dissipative particle dynamics study. Microfluidics and Nanofluidics, 2011, 10, 977-990.	2.2	31
65	Electroosmotic flow in a nanofluidic channel coated with neutral polymers. Microfluidics and Nanofluidics, 2010, 9, 1051-1062.	2.2	30
66	Encapsulation of dye molecules into mesoporous polymer resin and mesoporous polymer-silica films by an evaporation-induced self-assembly method. Journal of Luminescence, 2010, 130, 512-515.	3.1	5
67	Preparation and humidity sensitive property of mesoporous ZnO–SiO2 composite. Sensors and Actuators B: Chemical, 2010, 149, 413-419.	7.8	74
68	H2S-sensing properties of Pt-doped mesoporous indium oxide. Applied Surface Science, 2010, 256, 5051-5055.	6.1	35
69	Yttrium Oxide Nanowires. , 2010, , .		3
70	Rh–RhSxnanoparticles grafted on functionalized carbon nanotubes as catalyst for the oxygenreduction reaction. Journal of Materials Chemistry, 2010, 20, 736-742.	6.7	37
71	The study of photoluminescence properties of Rhodamine B encapsulated in mesoporous silica. Materials Chemistry and Physics, 2009, 118, 273-276.	4.0	48
72	Humidity sensitive property of Li-doped 3D periodic mesoporous silica SBA-16. Sensors and Actuators B: Chemical, 2009, 136, 392-398.	7.8	43

#	Article	IF	CITATIONS
73	Study on humidity sensitive property of K2CO3-SBA-15 composites. Applied Surface Science, 2009, 256, 280-283.	6.1	18
74	Facile Hydrothermal Synthesis of Yttrium Hydroxide Nanowires. Crystal Growth and Design, 2009, 9, 978-981.	3.0	35
75	Humidity-sensitive property of Fe2+ doped polypyrrole. Synthetic Metals, 2009, 159, 2469-2473.	3.9	37
76	Controlling the morphology of yttrium oxide through different precursors synthesized by hydrothermal method. Journal of Solid State Chemistry, 2008, 181, 1738-1743.	2.9	58
77	Synthesis and photoluminescent properties of mesoporous (MgO)x(ZnO)1â^'x materials. Materials Research Bulletin, 2008, 43, 601-610.	5.2	10
78	Synthesis of cluster polyaniline nanorod via a binary oxidant system. Materials Science and Engineering C, 2007, 27, 695-699.	7.3	17
79	Effect of polymerization time on the humidity sensing properties of polypyrrole. Sensors and Actuators B: Chemical, 2007, 125, 114-119.	7.8	74
80	Humidity sensitive property of Li-doped mesoporous silica SBA-15. Sensors and Actuators B: Chemical, 2007, 127, 323-329.	7.8	82
81	Blue-shifting photoluminescence of Tris (8-hydroxyquinoline) aluminium encapsulated in the channel of functionalized mesoporous silica SBA-15. Materials Chemistry and Physics, 2006, 100, 128-131.	4.0	28
82	Synthesis of metallic nanotube arrays in porous anodic aluminum oxide template through electroless deposition. Materials Research Bulletin, 2006, 41, 1417-1423.	5.2	64
83	Synthesis of alumina nanowires and nanorods by anodic oxidation method. Materials Letters, 2006, 60, 2937-2940.	2.6	25
84	Humidity sensitivity of polypyrrole and polypyrrole/SBA-15 host–guest composite materials. Journal of Applied Polymer Science, 2006, 102, 3301-3305.	2.6	24
85	Mesoporous silica tubes fabricated with human hair as template. Materials Chemistry and Physics, 2005, 91, 223-226.	4.0	4
86	Template synthesis of boron nitride nanotubes in mesoporous silica SBA-15. Materials Letters, 2005, 59, 925-928.	2.6	13
87	Synthesis of Higher Aluminum Content Hexagonal and Cubic Mesoporous Aluminosilicates toward Catalysts. Topics in Catalysis, 2005, 35, 25-34.	2.8	2
88	Electroless deposition of open-end Cu nanotube arrays. Solid State Communications, 2004, 132, 841-844.	1.9	42
89	Synthesis and humidity sensitivity of conducting polyaniline in SBA-15. Journal of Applied Polymer Science, 2004, 93, 1597-1601.	2.6	52
90	Host–guest composite materials of LiCl/NaY with wide range of humidity sensitivity. Materials Letters, 2004, 58, 1535-1539.	2.6	26

#	Article	IF	Citations
91	Understanding of the High Hydrothermal Stability of the Mesoporous Materials Prepared by the Assembly of Triblock Copolymer with Preformed Zeolite Precursors in Acidic Media. Journal of Physical Chemistry B, 2003, 107, 7551-7556.	2.6	73